Datashare 58:

A model describing flowback chemistry changes with time after Marcellus Shale hydraulic fracturing

Victor N. Balashov, Terry Engelder, Xin Gu, Matthew S. Fantle, and Susan L. Brantley

AAPG Bulletin, v. 99, no. 1 (January 2015), pp. 143–154

Strontium Isotope Analysis ($^{87}\mathrm{Sr}/^{86}\mathrm{Sr}$)

All isotope samples were processed in the Metal Isotope Laboratory (MIL) at Pennsylvania State University (Penn State). Pore fluids (from the soils) or digestates (of solid phase samples of Bald Eagle core or soil samples) were first filtered through 0.45 µm nylon syringe filters, dried down, resuspended in 3 N $\mathrm{HNO_3}$, and centrifuged. The resulting supernatant was pipetted off and an aliquot loaded onto an ion exchange column in 3 N $\mathrm{HNO_3}$. Solid samples were digested in a mixture of concentrated HF, $\mathrm{HNO_3}$, and $\mathrm{HClO_4}$, after breaking down organics in an initial 6 N nitric acid digestion on a hot plate at 90°C (194°F). The HF-$\mathrm{HNO_3}$-$\mathrm{HClO_4}$ digestate was dried and resuspended in HCl multiple times to ensure that no insoluble fluoride salts remained. Solutions were subsequently treated with a mixture of 30% $\mathrm{H_2O_2}$ and 4 N $\mathrm{HNO_3}$ to break down any remaining organics.

Aliquots of all samples were purified chromatographically using Eichrom Sr Spec resin; in some cases, samples were passed multiple times through the column to remove rubidium (Rb). Procedural blanks in the MIL clean laboratory facilities are typically $\ll$ 0.5 ng Sr, which is $\ll$ 0.5% of the total sample mass processed.

Measurements of Sr isotopic composition ($^{87}\mathrm{Sr}/^{86}\mathrm{Sr}$) were conducted using a Thermo Scientific Neptune Plus multiple collector ICP-MS (MC-ICP-MS) in the MIL. All solution concentrations were matched to the SRM-987 standard (200 ppb Sr), which was run multiple times during an analytical session. The solution uptake rate was ~33 µl $\mathrm{min^{-1}}$ using an ESI PFA micronebulizer and wet plasma conditions at low mass resolution.

Both $^{82}\mathrm{Kr}$ (11.593%) and $^{83}\mathrm{Kr}$ (11.5%) were measured during each analysis, as Kr is a low-level contaminant found in most liquid Ar sources, Kr unresolvably interferes isobarically at masses 84 ($^{84}\mathrm{Kr} = 56.987\%$) and 86 ($^{86}\mathrm{Kr} = 17.279\%$). A typical ion beam voltage for $^{88}\mathrm{Sr}$ (200 ppb Sr solution) is ~9 – 10 V (0.05 V/ppb), whereas $^{82}\mathrm{Kr}$ and $^{83}\mathrm{Kr}$ are typically 0.1 to 0.2 mV. All data are corrected for Kr interferences by calculating the extent to which the Kr is fractionated from its expected value (1.008) using an exponential law:

Table S1. Composition of Marcellus Shale (Bald Eagle Core) and Leachate Samples

Sample	Na	K	Mg	Ca	Sr	Ba	Mn	Fe	Al	Si	P	Ti
Concentration in shale (µmoles per gram shale)												
BE850*	204.8	726.2	377.6	989.7	2.52	8.39	4.14	739.2	3111.7	9119.4	18.45	96.26
BE874*	233.6	749.8	349.0	431.0	1.92	7.94	3.59	719.2	3060.7	10137.2	14.82	95.15
Concentration in leachate (µmoles in leachate per gram shale)												
BE850	13.77	2.52	0.55	3.44	0.036	0.030	BDL†	BDL	BDL	BDL	0.34	BDL
BE874	15.90	4.05	0.95	5.06	0.044	0.019	BDL	BDL	BDL	(1.58)	0.54	BDL
Ratio of element in leachate with respect to Ca												
BE850	4.01	0.73	0.16	1	0.01	0.009	BDL	BDL	BDL	BDL		BDL
BE874	3.14	0.80	0.19	1	0.009	0.004	BDL	BDL	BDL			BDL

*Depth of sample below land surface (in feet) noted as sample number.

†BDL, below detection limit.

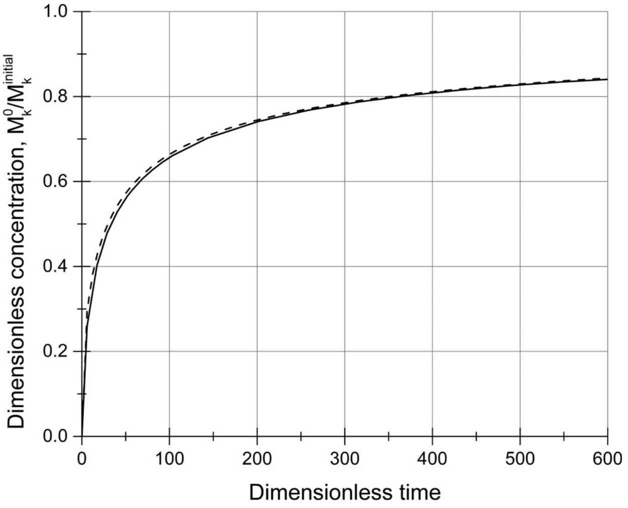

Figure S1. Comparison of the numerical solution in dimensionless form (solid line) described in text with the approximate analytical solution (dashed line) by Crank (1980).

$$\left(\frac{{}^{i}X}{{}^{j}X}\right)_{\text{meas}} = \left(\frac{{}^{i}X}{{}^{j}X}\right)_{\text{actual}} \left(\frac{m_i}{m_j}\right)^{p}$$

in which ${}^{i}X$ indicates nuclide i, and m is the atomic mass of nuclide i. The derived p-value is used to calculate accurate ^{84}Kr and ^{86}Kr ion beam intensities, which are not resolvable from the ^{84}Sr and ^{86}Sr ion beams on the Neptune. The fractionation-corrected values are then used to correct the measured data at masses 84 and 86; all Sr isotope ratios are then

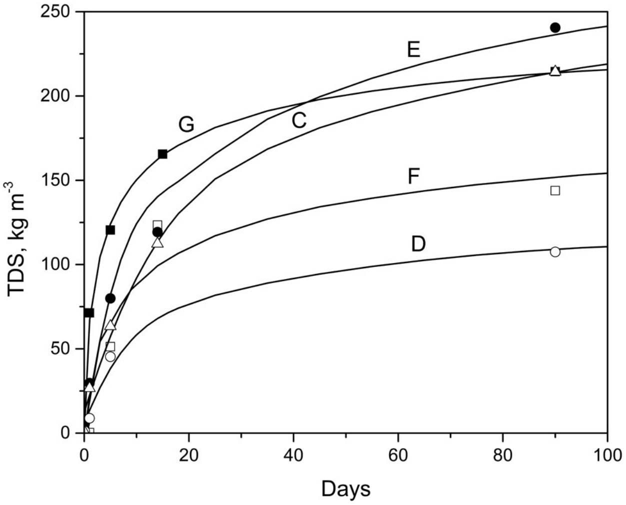

Figure S3. The change over 100 days for the concentrations of total dissolved solids in five horizontally drilled and hydrofractured wells (different data symbols refer to wells C, D, E, F, and G) (Hayes, 2009). Lines represent model outputs in which the value of b_1 and the initial total concentration was fit to the time-series data for each well as described in the text.

Figure S2. The concentrations of the pore brine species in the shale plotted at different times as the salts diffuse from the matrix into a planar fracture of 90.64 mm (3.6 in.) aperture. The fracture wall is located at $x = 0$. NaCl, $CaCl_2$, and $MgCl_2$ diffuse from the matrix (porosity 2%) to fracture at 75°C (167°F) and 30 MPa (4350 psi). The brine diffusion coefficient (D^{aq}) and inverse Archie factor of the matrix (F_{inv}) were set to 3.77×10^{-9} m^2 s^{-1} and 1.8×10^{-3}, respectively.

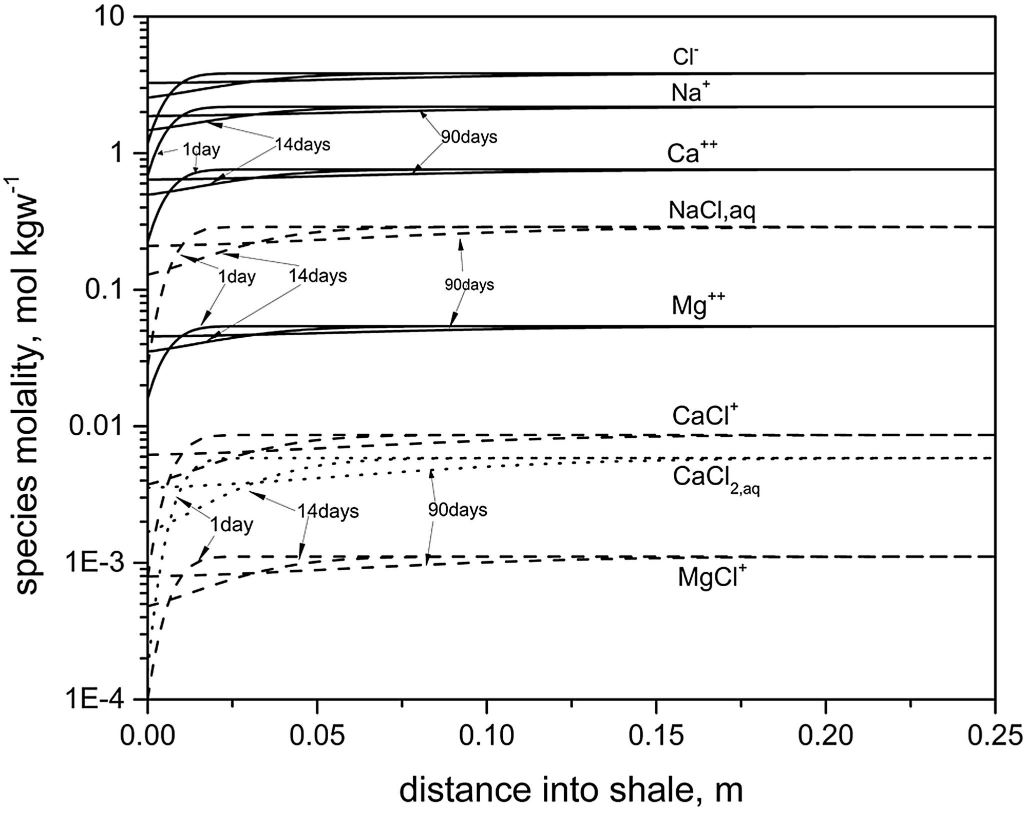

Table S2. Initial Equilibrium Speciation of Injected Treatment Water and Pore Brine

Chemical Entity	Fracture fluid	Pore Brine (Well G)
	Molality, mol kgw^{-1}	
Na^+	1.58×10^{-3}	2.233
K^+	1.3×10^{-4}	1.254×10^{-3}
Mg^{++}	1.5×10^{-4}	4.438×10^{-2}
Ca^{++}	1.035×10^{-3}	7.591×10^{-1}
Fe^{++}	1.2×10^{-5}	1.517×10^{-14}
$Al(OH)_3{}^{\circ}$	1.134×10^{-7}	5.825×10^{-10}
$SiO_2{}^{\circ}$	9.684×10^{-7}	1.889×10^{-4}
SO_4^-	6.097×10^{-4}	6.878×10^{-4}
Cl^-	2.46×10^{-3}	3.835
$CO_2{}^{\circ}$	7.956×10^{-6}	6.313×10^{-5}
$NaCl^{\circ}$	1.332×10^{-7}	2.937×10^{-1}
KCl°	3.921×10^{-9}	5.898×10^{-5}
$MgCl^+$	1.979×10^{-9}	9.128×10^{-4}
$CaCl^+$	7.552×10^{-9}	8.634×10^{-3}
$CaCl_2{}^{\circ}$	3.272×10^{-12}	5.832×10^{-3}
Fe^{+++}	8.451×10^{-16}	1.011×10^{-27}
$Al(OH)_4^-$	1.089×10^{-5}	1.269×10^{-8}
HCO_3^-	3.813×10^{-4}	6.844×10^{-4}
CO_3^-	1.177×10^{-5}	4.804×10^{-6}
$NaSO_4^-$	2.904×10^{-7}	4.633×10^{-4}
$Na_2SO_4{}^{\circ}$	5.558×10^{-10}	1.254×10^{-3}
$NaCl + KCl + CaCl_2 + MgCl_2$	2.9×10^{-3}	3.347
pH	7.324	6.679
E_h (V)	–0.094	–0.303
$V_w(dm^3\ kgw^{-1})$	1.013	1.026
	kg m^{-3}	
Total dissolved solids	0.228	237.93

Table S3. $^{87}Sr/^{86}Sr$ Values of Core, Soil, and Pore Fluid Samples

Sample	$^{87}Sr/^{86}Sr$[*]	Interference-Corrected Ratios		$^{82}Kr/^{83}Kr_{meas}$
		$^{87}Sr/^{86}Sr$[†]	$^{87}Sr/^{86}Sr$[‡]	
Pore fluids				
VF 40 cm[§]	0.730867	0.730869	0.730712	2.389
VF 50 cm[§]	0.728007	0.728014	0.727708	2.169
VF 80 cm[§]	0.727053	0.727063	0.726992	2.015
Solids				
VF7[¶]	0.749981	0.750011	0.749994	1.453
VF13[#]	0.751265	0.751293	0.751271	1.540
VF13 repl[**]	0.751288	0.751318	0.751269	1.506
BE810.5[††]	0.730024	0.730053	0.730034	1.516
BE850[‡‡]	0.722943	0.722974	0.722959	1.471

[*] No interference correction applied, mass bias corrected. Internal standard error = 0.000003 for all analyses.

[†] Kr correction applied (see text for description).

[‡] Kr and Rb corrections applied (see text for description).

[§] Soil pore fluids sampled at depths shown from the valley floor site (Jin et al., 2013).

[¶] Valley floor soil sampled from 45 to 52 cm depth near Huntingdon, Pennsylvania (Jin et al., 2013).

[#] Valley floor soil sampled from 77 to 82 cm depth near Huntingdon, Pennsylvania, (Jin et al., 2013).

[**] VF13 replicate.

[††] Shale sample from 810.5 feet bls in the Bald Eagle core drilled at Howard, Pennsylvania.

[‡‡] Same as (††), but from 850 feet bls.

corrected for mass bias by internal normalization using an exponential law and an assumed $^{86}Sr/^{88}Sr$ of 0.1194. Typical Kr corrections are less than 0.000010 on the $^{87}Sr/^{86}Sr$ ratio.

Rubidium, which interferes at mass 87, is monitored at mass 85 (^{85}Rb) in each analysis. Systematic laboratory tests have shown that Rb concentrations up to at least 250 ppt ($^{85}Rb/^{88}Sr \sim 0.001$) are correctable using the same exponential correction factor (p) for Rb as for Sr. In a series of Rb-doped SRM-987 solutions, the recovered $^{87}Sr/^{88}Sr$ after Kr and Rb corrections was 0.710244 ± 0.000027 (1SD), well within the certified range (0.71034 ± 0.00026). Unless otherwise noted, the $^{87}Sr/^{86}Sr$ ratios reported have no Rb correction applied. For completeness and clarity, both the Rb-corrected and uncorrected $^{87}Sr/^{86}Sr$ ratios are reported in Table S3, along with measured $^{87}Sr/^{86}Sr$ and Kr-uncorrected $^{87}Sr/^{86}Sr$.

Measurements of the NIST standard reference material (SRM) 987 yielded $^{87}Sr/^{86}Sr$ values of 0.710239 ± 0.000012 (1SD, $n = 12$) over the period during which the samples were measured, well within the certified range of 0.71034 ± 0.00026. Purified natural seawater samples (~0.70914, $n = 2$; IAPSO: 0.709156–0.7092) and rock standards (e.g., BCR-1: 0.705012 ± 0.00001 with no Rb correction and 0.705000 ± 0.000001 with a Rb correction, $n = 2$; 0.705 literature value) are also within error of accepted values.

REFERENCES CITED

Crank, J., 1980, The Mathematics of Diffusion: Oxford, Oxford: University Press, 432 p.

Hayes, T., 2009, Sampling and analysis of water streams associated with the development of Marcellus shale gas, Marcellus Shale Coalition: Des Plaines, Illinois, Gas Technology Institute, 80 p., www.bucknell.edu/MarcellusShaleDatabase.

Jin, L., R. Mathur, G. Rother, D. Cole, E. Bazilivskaya, J. Williams, A. Carone, and S. Brantley, 2013, Evolution of porosity and geochemistry in Marcellus Formation black shale during weathering: Chemical Geology, v. 356, p. 50–63.